Corrosion Resistance of Friction Stir Welded AA6061 Aluminium Alloy

K.Ratnakumar[1], G. Madhusudhan Reddy[2] and K.Srinivasa Rao[3]
[1]Department of Metallurgical Engineering, Government Polytechnic, Visakhapatnam – INDIA. [2]Defence Metallurgical Research Laboratory; Hyderabad, INDIA. [3]Department of Metallurgical Engineering, Andhra University College of Engineering (A), Visakhapatnam- 530 003, INDIA. Email : arunaraok@yahoo.com

ABSTRACT

Present work pertains to microstructure and the corrosion behaviour of the nugget zone (NZ), thermo mechanically affected zone (TMAZ) and heat affected zone (HAZ) of friction stir welded AA6061 alloy. An attempt was made to find the influence of prior thermal temper of the alloy. Potentio-dynamic polarisation testing was used to determine the pitting corrosion resistance of the welds. Optical microscopy (OM) and transmission electron microscopy (TEM) with Energy dispersive X-ray spectroscopy studies were carried out to find the mechanism of formation of TMAZ and corrosion. Friction stir welding of this alloy resulted in fine recrystallized grains in weld nugget which has been attributed to frictional heating and plastic flow. The process also produced a softened region in the weld nugget, which may be due to the dissolution and growth of possible precipitates. Corrosion resistance of nugget zone has been found to be higher than that of TMAZ and base metal. Corrosion resistance of naturally aged (T4) alloy exhibit higher corrosion resistance than that of artificial aged (T6) alloy.

Keywords: Pitting corrosion, General corrosion, Dynamic polarisation, Friction stir welding, Aluminium alloys.

1.0 INTRODUCTION

Friction stir welding (FSW) is a revolutionary solid state welding technique that is progressing rapidly as a manufacturing and assembly process for joining aluminum alloys, magnesium alloys and stainless steels. This process is beginning to provide breakthrough reductions in the manufacturing costs of both non-aerospace and aerospace systems. The rapid implementation of FSW has been enabled by the ability to utilize processing equipment based on traditional machine tool technologies and the capability to produce traditional metallurgical joints with "parent" metal soundness. For the successful implementation of FSW, there is much room for improvement, particularly in the area of metallurgical understanding of the process which results in the various microstructural features schematically illustrated in **Fig. 1.** Friction stir welding produces a far less heterogeneous microstructure than conventional fusion welding. It results in three microstructural regions: the nugget, where the material has undergone severe stirring and heating, the thermo-mechanically affected zone (TMAZ) which is subjected to both deformation and heating, and the heat affected zone (HAZ) where the material experiences only a thermal cycle. Microscopically, these regions are significantly different, especially in heat-treatable aluminum alloys, magnesium alloys and stainless steels.

Generally melting does not occur during FSW, but temperatures are sufficiently high enough to cause dissolution, nucleation and coarsening of strengthening precipitates in heat treatable Al-alloys. Microstructure and mechanical properties of friction stir welded 6013 alloy was investigated by B.Heinz, et. al [1]. Friction stir welding caused dynamic recrystallization in the weld nugget resulting in smaller and
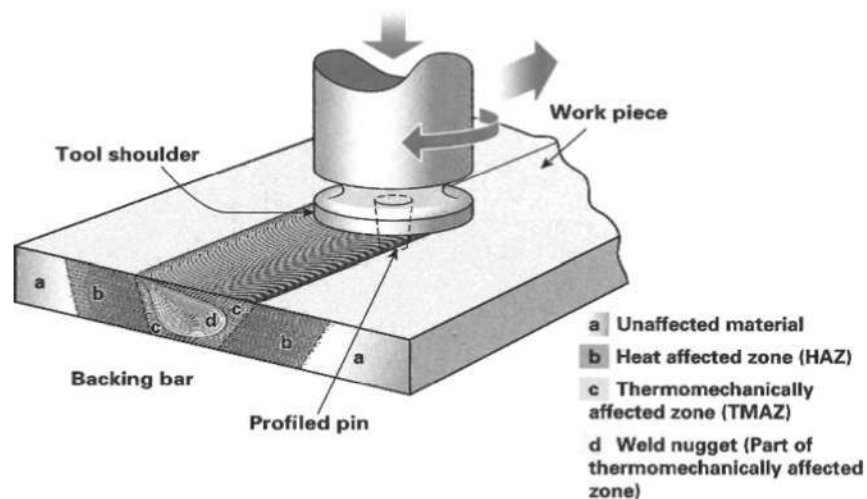
Fig. 1 : Different zones of Friction stir weld joint

equiaxed grains as compared to the larger elongated grains of the base material. The grain size of the heat-affected zone is retained. The strengthening precipitates in the weld are dissolved while those in heat-affected zone coarsened considerably. The altered microstructure in the weld zone leads to sensitization in the as welded condition. The study focused on microstructures in FSW Al alloy AA 7075-T651, an alloy not commonly fusion welded, revealed corrosion susceptibility [2]. Although the heat input associated with FSW was relatively low and the time at temperature was short compared to fusion welding, localized microstructures, chemical segregation, and precipitate distributions were created that generally are not present in parent metal AA7075-T651. The results provided evidence that the lowered resistance to intergranular corrosion following FSW of AA7075-T651 was caused by a difference in pitting potentials. The susceptibility of welded and unwelded samples of Al-Mg alloy to pitting corrosion and stress corrosion cracking (SCC) in chloride solutions was studied by Frankel and Xia [3]. The FSW samples exhibited superior resistance to pitting corrosion compared to the base metal and arc-welded samples. The general corrosion, pitting and stress corrosion cracking (SCC) resistance of Al-Cu-Li alloy AA2195 plates joined by FSW was investigated by Hu and Meletis, [4]. Plates of Al-Cu alloy AA2219 joined by FSW were also tested for comparison purposes along with AA2195. Alloy 2195 was found to be more resistant to environmental cracking than 2219. The microstructure, the microchemistry and the environmental assisted cracking susceptibility was investigated for friction stir welded AA2219-T87 plates [5]. It was found that the coarsening of the Al_2Cu intragranular

precipitates occurring within the thermo-mechanically and the heat affected zones after friction stir welding. The corrosion immersion tests indicated an increased resistance to corrosion for the friction stir welded region as compared to the weld unaffected parent metal. The corrosion behaviour of a friction stir welded AA7108-T79 aluminium alloy has been investigated using accelerated testing (ASTM G34 EXCO) and electro-chemical measurements [6]. Corrosion testing revealed that the edge regions of the thermo-mechanically affected zone were most susceptible to corrosion. The localized corrosion occurs intergranularly due to the non-uniform distribution of ç ($MgZn_2$) precipitates within the thermomechanically affected zone. Work of Lumseden et al., has shown that the composition changes caused by the nucleation and coarsening of precipitates during FSW produce a sensitized microstructure in AA7050 and AA7075 aluminum alloys and are susceptible to intergranular corrosion and SCC [7]. Above limited literature available indicated that FSW Al-alloys are susceptible to corrosion. Present study is aimed at studying the effect of prior thermal temper on pitting corrosion behaviour of various zones of FSW AA6061 alloy.

2.0 EXPERIMENTAL METHODS

Wrought AA6061 alloy plates of thickness 6mm in T6 (solution treatment at 540°C for 1h and aged at 160°C for 12 h) and T4 (solution treatment at 540°C for 1h and aged at room temperature for 30 days) tempers were used for friction stir welding. The chemical composition of the base metal was given in **Table 1**. The parameters used for the friction stir welding are given in the **Table 2**.

Table 1 :   Composition and constituents (wt%) of the base metal AA6061

Element	Wt. percentage
Mg	0.689
Si	0.531
Fe	0.230
Mn	0.331
Cu	0.305
Available Si	0.390

Table 2 :   Tool size and welding parameters used in experiments

Tool Size			Welding parameters	
Shoulder Speed Diameter (mm)	Pin diameter (mm)	Pin length (mm)	Rotation speed (rev min^{-1})	Travel (mm min^{-1})
10	5	6.4	1000	15

The weld bead was made perpendicular to the sheet rolling direction with full depth of penetration i.e., 6mm. The macrostructures of the top and bottom view of a typical joint of FSW AA6061 alloy was given in **Fig. 2**. The microstructures were recorded with an image analyzer attached to the metallurgical microscope. Transmission electron microscopy (TEM) with Energy dispersive X-ray spectroscopy (EDXS) was done on base metal, nugget zone and thermomechanically affected zone. A software based PAR electrochemical weld tester system was used to carry out potentiodynamic polarization tests to study the pitting corrosion behavior of the base metal, weld metal, HAZ and TMAZ regions. A saturated calomel electrode (SCE) and carbon electrode were used as reference and auxiliary electrodes respectively. All experiments were conducted in aerated 3.5% NaCl solutions with pH adjusted to 10 by adding potassium hydroxide. The potential
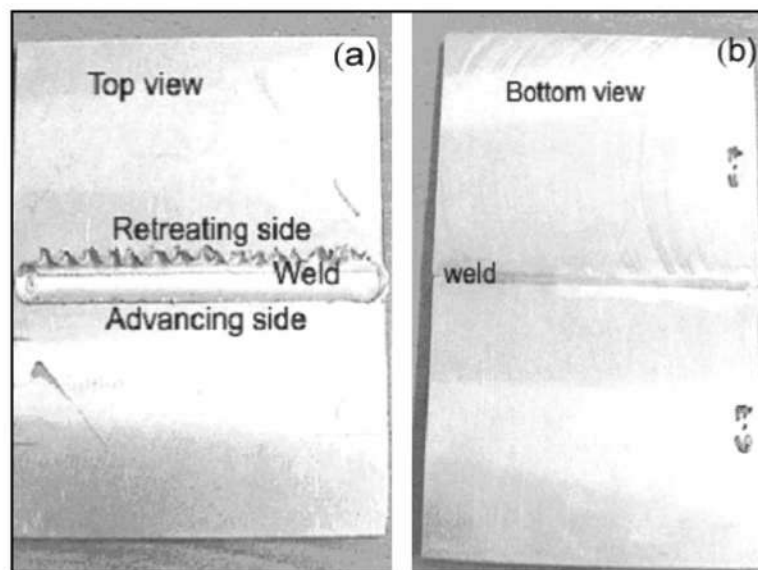

Figure 2 : Top and Bottom views of the AA6061 Friction Stir welds

scan was carried out at 0.166 mVs^{-1} with the initial potential 0f −0.25 V (OC) SCE to the final pitting potential. The exposure area for these experiments was 0.6 cm^2. The potential at which current increased drastically was considered to be the critical pitting corrosion E$_{pit}$. Specimens exhibiting relatively more passive potential (or less negative potentials) were considered to have better pitting corrosion resistance. The pitting potentials of base metal and various zones of friction stir welded T4 and T6 AA6061 alloy were recorded. Optical microscopy on dynamically polarized samples was carried out to understand the mechanism of pitting.

3.0 RESULTS AND DISCUSSION

3.1 Base metal studies

Optical micrographs of the base metals AA6061-T4 and AA6061-T6 are shown in **Fig. 3**. The grain structure was well developed and grains of AA6061-T6 are slightly coarser than that of AA6061-T4. Micrographs revealed that more number of Mg$_2$Si particles were present in artificially aging (T6) alloy when compared to that of naturally aged alloy (T4).
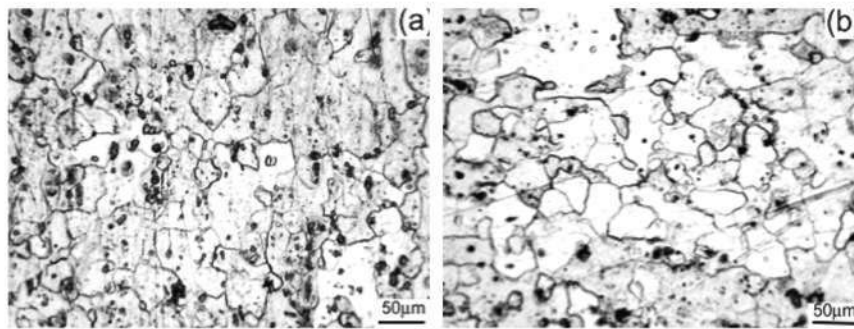

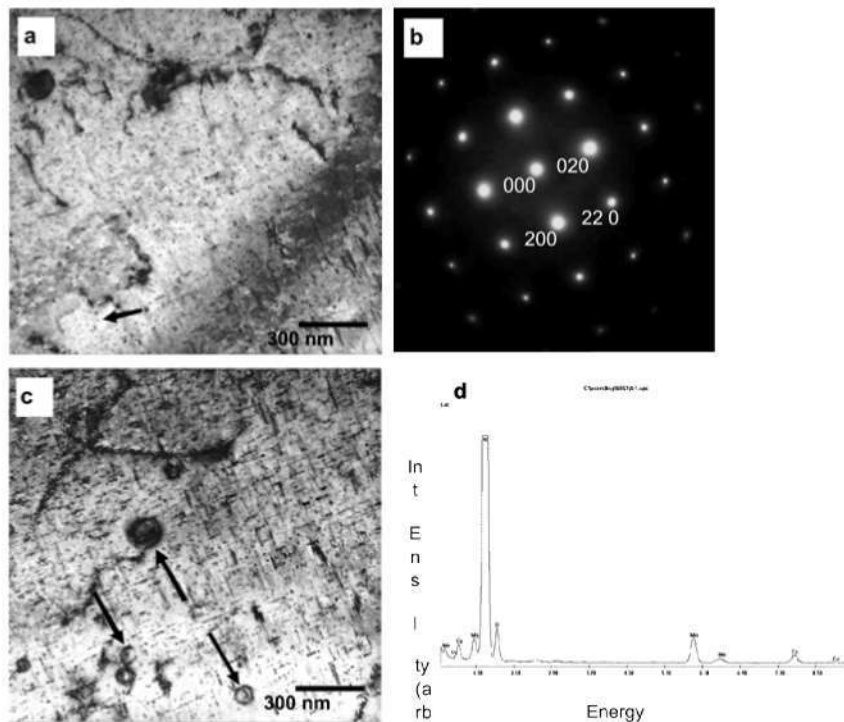Fig. 3 : Optical micrographs of AA6061 alloy (a) T4 Condition (b) T6 Condition

Fig. 4 : (a) TEM bright field image showing the general microstructure of the base alloy consisting of Mg2Si metastable precipitates in <001> zone axis. (b) Selected area electron diffraction obtained from (a). (c) Bright field image showing few Mn containing particles (arrow marked). (d) Energy dispersive X-ray spectrum (EDXS) collected from the particles shown in (c).

Fig. 4 shows TEM images of microstructure of base metal. It consisted of metastable precipitates Mg_2Si with uniform dislocations distribution within the grain. Presence of precipitates is confirmed with selected area electron diffraction and Energy dispersive X-ray spectrum.

3.2 Microstructural studies of FSW joint

Optical micrographs of various zones of FSW AA6061 in T6 condition is shown in the **Fig. 5**. The weld nugget has a recrystallized, fine equiaxed grain structure. This indicates that, during the process of FSW, the precipitates have dissolved into the solution and reprecipitated on subsequent cooling. The recrystalization of the weld nugget and the redistribution of the precipitates indicate that the temperature obtained during the process is above the solutionizing temperature but below the melting temperature of the alloy [8]. The finer precipitates are absent in weld nugget because the cooling rates are such that larger precipitates could nucleate and grow but not the finer ones.

TMAZ is the transition zone between the base metal and the weld nugget, characterized by a highly deformed structure as shown in **Fig. 5c**. Optical micrograph shows a banded structure. There is no recrystalization in this region. There is no significant change in the size and morphology of coarser precipitates, but their orientation is along thickness direction which is similar to rolling direction in parent metal. The

precipitates are quite random. The finer precipitates observed in parent metal are coarsened during welding.

A static evaluation of the grain size has been carried out on the base metal in T6 and the weld nugget zone areas. In the base metal the mean grain size was $65\mu m$ and clearly preferentially along the rolling direction. Weld-nugget zone is characterized by the presence of equiaxed grains finer than that of base metal whose mean size was $10\mu m$. The presence of fine grain size is due to the dynamic recrystallization occurred during the welding.

During FSW, the original grains and sub grains of the base material seemed to be formed with finer, equiaxed grains formed by a recrystallization mechanism because of high strain rates involved in this process. **Fig. 6** illustrates the major microstructure changes in the weld nugget zone. A higher number of fine and little hardening Mg_2Si precipitates is evident. **Fig. 6b** illustrates a detail of the inner part of a recrystallized grain and reveals clearly the evidence of precipitates at the grain boundary region. Temperature in the thermo mechanically affected zone is higher in the advancing side compared to that of retreating side. TEM images of advancing side (**Fig. 7c** and **Fig. 7d**) clearly indicated coarsened precipitates and reduction in the dislocation density compared to that of retreating side (**Fig. 7a** and **Fig. 7b**).
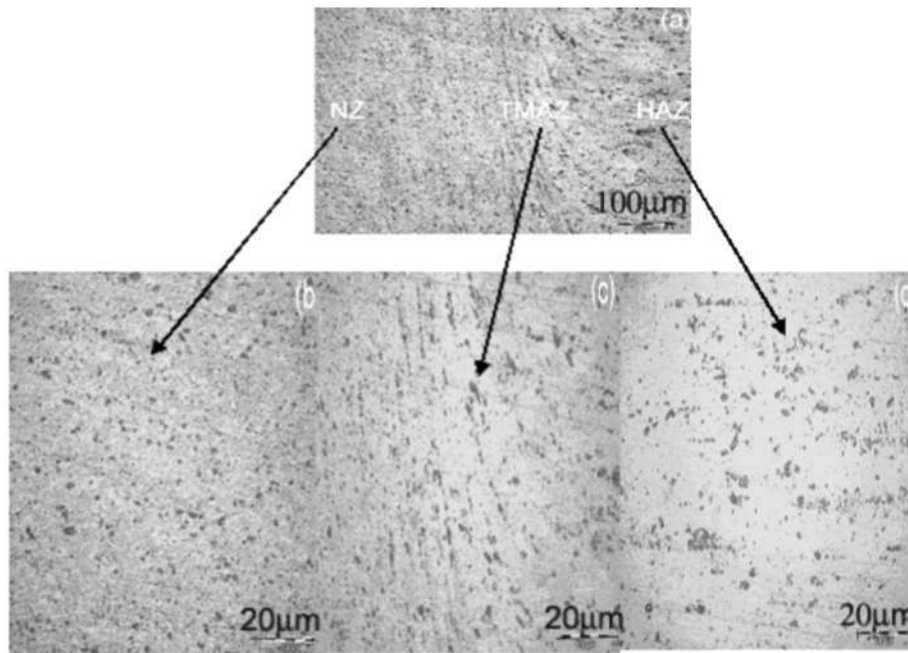

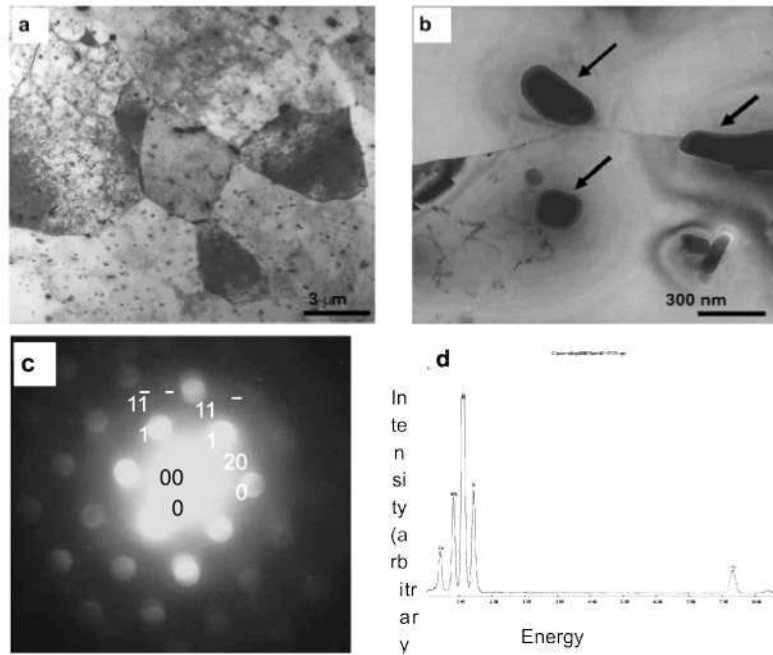**Fig. 5 : Optical micrographs of various zones of FSW AA6061-T6 alloy**

45

Fig. 6 : (a) TEM bright field image showing the microstructure of the weld pool consisting of fine recrystallized grains of alumjinium with Mg$_2$Si precipitates. **(b)** Bright field image showing equilibrium Mg$_2$Si precipitates (arrow marked) at higher magnification.
(c) Micro diffraction pattern obtained from the Mg$_2$Si particles corresponds to <011> zone axis of FCC with an average lattice parameter of a = 0.64 nm.
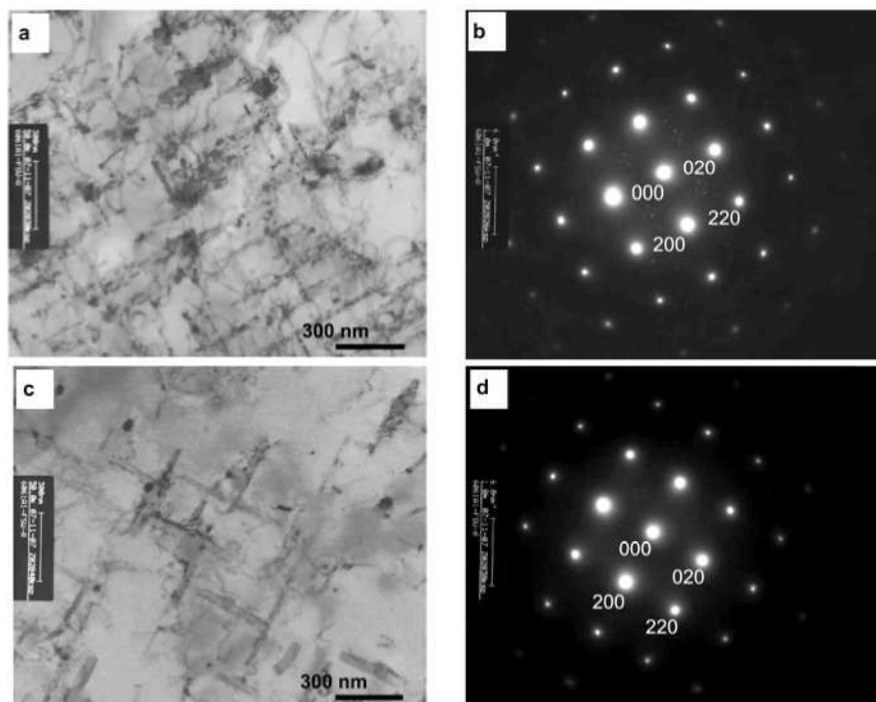**(d)** Energy dispersive X-ray spectrum (EDXS) collected from the particles shown in (b)

Fig. 7 : (a) & (c) TEM bright field image showing the microstructure at the retracting and advancing sides of the weld respectively consisting of metastable Mg$_2$Si precipitates. in <001> direction. **(b) & (d)** Selected area electron diffraction obtained from (a) and (c) respectively consisting of diffraction spots belongs to Mg$_2$Si precipitates

3.3 Pitting corrosion studies

The potentiostatic polarization curve for base metal in T4 and T6 conditions are given in **Fig. 8**. The pitting potentials of the base metals in T4 and T6 condition was given in **Table 3**.
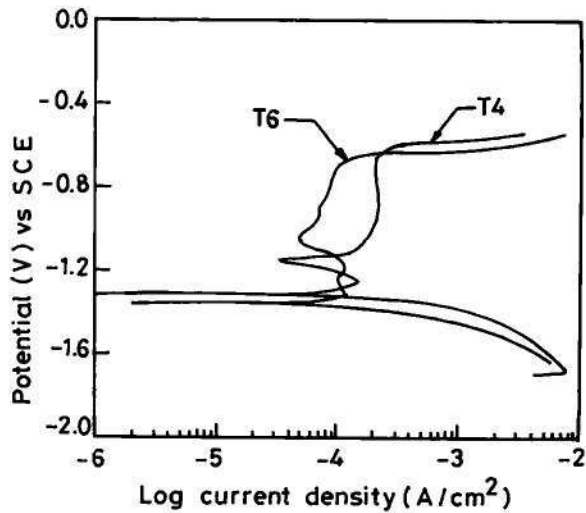

Fig. 8 : Potentiodynamic polarization curves of AA6061 alloy

Table 3 : Epit values of base metal AA6061 alloy

Prior thermal temper	Epit values (mV)
T4	-613
T6	-688

Base metal in T4 condition shows high pitting corrosion resistance than that of T6 condition. The potentiodynamic polarization curves for FSW AA6061-T4 and T6 in the zones of WN, TMAZ and HAZ are given in **Fig. 9** and **Fig. 10**. The critical pitting potentials of test specimens **(Table 4)** clearly indicated a greater pitting corrosion resistance of weld metal than base metal. This is attributed to the precipitates present in the alloy promote matrix dissolution through selective dissolution of aluminum from the particle. These precipitate deposits are highly cathodic compared to the metallic matrix, which initiates pitting at the surrounding matrix and also enhances pit growth. During FSW only the coarser precipitates could nucleate and grow but not the finer ones. This aids in formation of passive film, which remained more intact on surface of the sample. Aging produces a microstructure of uniform distribution of precipitates in aluminum matrix. This condition creates inhomogeneity on a microscopic scale. The precipitates are noble and promote anodic dissolution of the matrix. The higher pitting corrosion resistance of the weld nugget can be attributed to the dissolution of the precipitates. Population of the precipitates is quiet low compared to the other areas because of the high temperature generation. The nugget area is more or less similar to solution treated condition of the aluminium alloy. The TMAZ shows a poor pitting corrosion resistance as compared to base metal. During FSW process this region heats up to a temperature just below the solutionizing
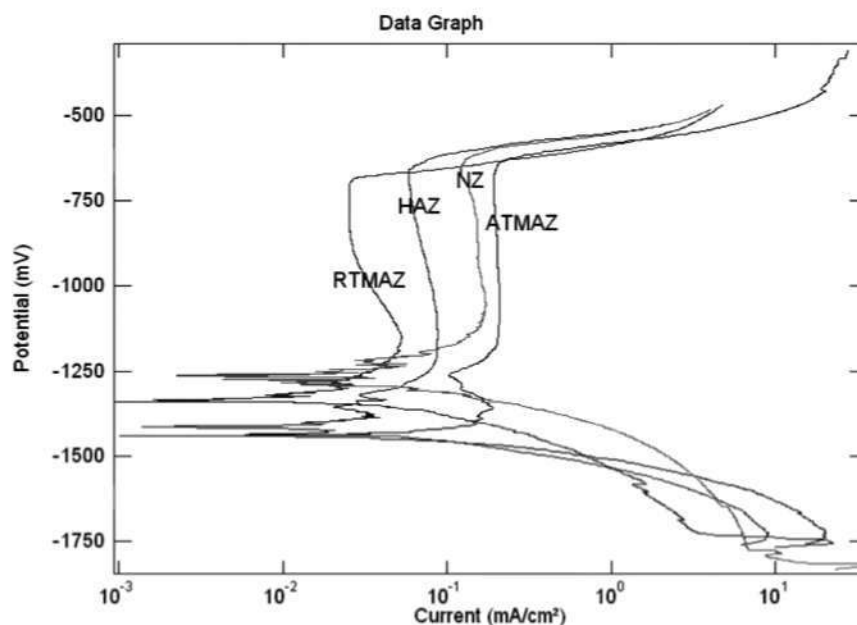

Fig. 9 : Potentiodynamic polarization curves of FS welded AA6061-T4 alloy

47

temperature of the alloy which results in coarsening of precipitates. The slightly more negative critical pitting potential of TMAZ than base metal can be attributed to the presence of residual stresses induced during the process of FSW [9].

The microstructures of pitted surfaces are shown in **Fig. 11**

and **Fig. 12** and it reveals clearly that pit density of weld region is much less than that of base metal and TMAZ. Hence it can be concluded that pitting resistance of weld region is higher than that of base metal and TMAZ. Pitting resistance of AA6061 is better in T4 condition compared to T6 condition.
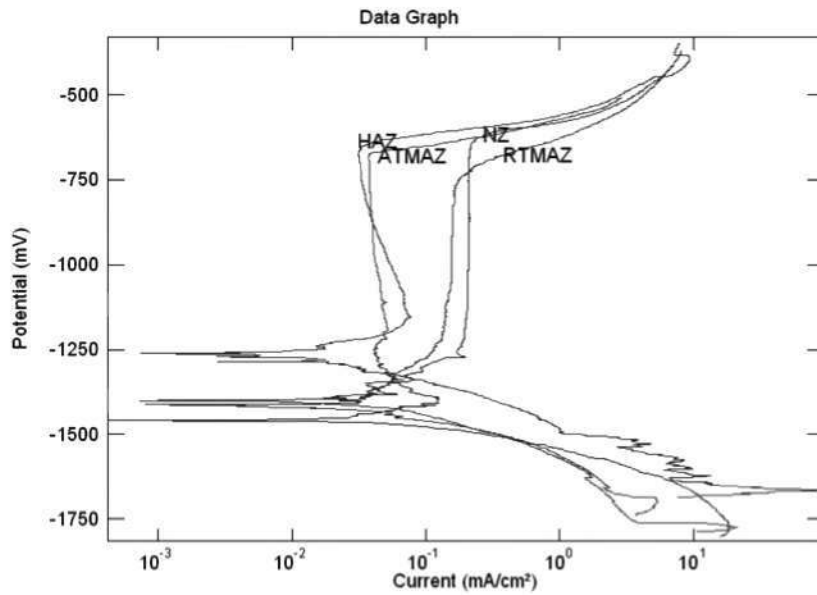

Fig. 10 : Potentiodynamic polarization curves of FS welded AA6061-T6 alloy

Table 4 :   Epit values of NZ, TMAZ, and HAZ of FSW AA6061 alloy

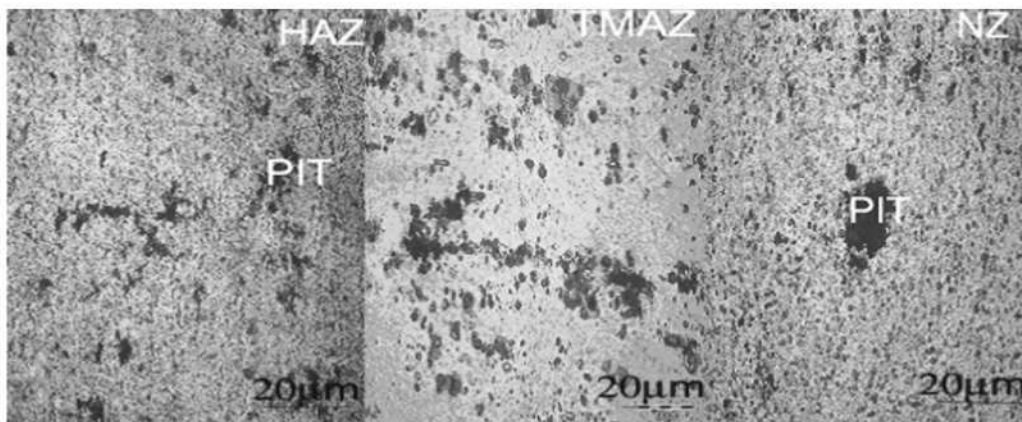| Zone	T4 (mV)	T6 (mV)
Nugget Zone	-581	-595
Advancing side of TMAZ	-625	-632
Retreating side of TMAZ	-630	-646
Heat Affected Zone	-633	-617

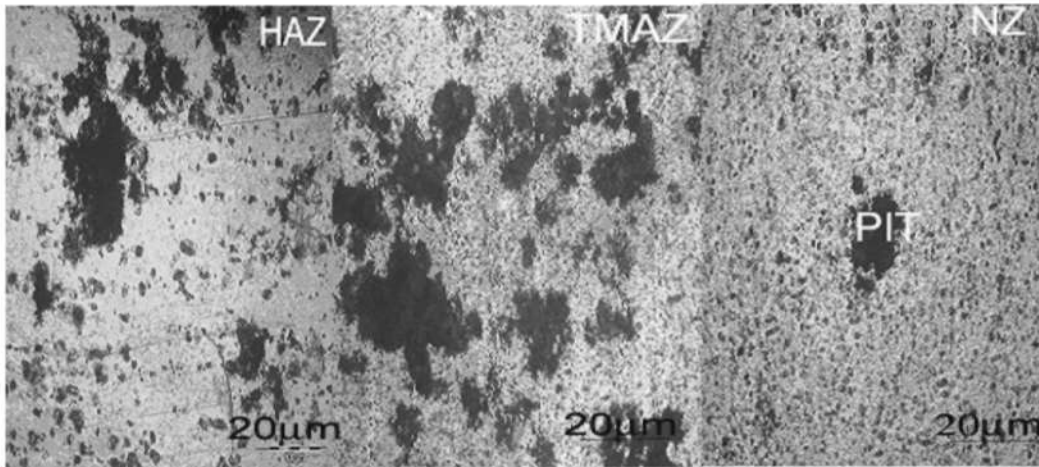Fig. 11 : Optical micrographs of FS welded AA6061-T4 alloy after corrosion

Figure12 : Optical micrographs of FS welded AA6061-T6 alloy after corrosion

4.0 CONCLUSIONS

Considerable grain refinement in weld nugget has been achieved and it may be due to dynamic recrystallization caused by high strain rates involved in this process. Pitting corrosion resistance of weld nugget is higher than that of thermo-mechanical affected zone and the base metal. This was attributed to dissolution of precipitates. Corrosion damage is more in the retreating side than the advancing side of FSW AA6061. Pitting corrosion resistance of FSW AA6061 alloy is higher in T4 condition compared to that of T6 condition.

REFERENCES

1 B. Heinz, B. Skrotzki and G. Eggeler (2000); Materials Science Forum, 331-337, p. 1757-1762.

2. J. M. Lumsden, M. W. Mahoney, G. A. Pollock, and C. G. Rhodes (1999): Corrosion, 55 (12), p. 1127-1135.

3. G. S. Frankel and Z. Xia (1999); Corrosion, 55 (2), p. 139-150.

4. W. Hu and E. I. Meletis (2000); Materials Science Forum, 331-337, p. 1683-1688.

5. C. S. Paglia and R. G. Buchheit (2006); Materials Science And Engineering, A 429, p. 107–114.

6. D. A. Wadeson a, X. Zhou a, G. E. Thompson, P. Skeldon and G. Scamans (2006); Corrosion science, 48, p. 887–897.

7. Jesse Lumsden, Gary. Pollock and Murraymahoney (2003); Material Science Forum, 426- 432, p. 2867-2872.

8. K. A. A. Hassan, P. B. Prangnell, A. F. Norman, D. A. Price and S. W. Williams (2003); Science and Technology of welding and joining, 8 (4), p. 257-268.

9. G. M. Reddy, P. Mohandas, P. Mastanaiah and C. V. S. Murthy (2006); Proc. National seminal Non-destructive evaluation, ,Indian Soceity of Non-destructive Testing, Hyderabad, p.1-7.